Engineering Structures 172 (2018) 131–140

Contents lists available at ScienceDirect

Engineering Structures

journal homepage: www.elsevier.com/locate/engstruct

# Experimental study on the axial compressive strength of vertical inner plate reinforced square hollow section T-joints

Hongfei Chang[a,b,*], Junwu Xia[a,b], Zhen Guo[b], Chao Hou[c], Wei Din[b], Fuyang Qin[b]

[a] State Key Laboratory of Geomechanics and Deep Underground Engineering, China University of Mining and Technology, Xuzhou, China
[b] School of Mechanics and Civil Engineering, China University of Mining and Technology, Xuzhou, China
[c] School of Civil Engineering, The University of Sydney, Sydney, NSW 2006, Australia

ARTICLE INFO

*Keywords:*
Compressive strength
Vertical inner plate
Reinforced joints
Square hollow section
Experimental test
Finite element analysis

ABSTRACT

To evaluate the influence of vertical inner plate reinforcement on the compression behavior of square hollow section joints, four T-joints with and without such reinforcement were tested experimentally and simulated numerically. The experimental set-up and failure sequences are described while the strain distribution, load-displacement curves, compressive strength as well as the failure modes of the joints are analyzed. The test results demonstrate that the vertical inner plate is effective to enhance the compressive strength of the SHS T-joints, yet the efficiency of the reinforcement decreases with the increase of the width ratio between the brace and the chord. Meanwhile, the presence of the vertical inner plate has little influence on the strain distribution and failure mode of the joint. The failure of the vertical inner plate reinforced T-joints is dominated by two modes, namely flange yielding and web buckling. The yielding of the chord flange will dominate for joints with small brace-chord width ratio, and the combination of flange yielding and web buckling will dominate for joints with large brace-chord width ratio. The numerical models of the specimens are developed and used to reveal the mechanism of the vertical inner plate to increase the compressive strength of the joint. The function of the vertical inner plate can be divided into two aspects, one is to enlarge the yielding scope at the top flange of the chord, and the other is to drive the yielding at the bottom flange of the chord. The proposed equation achieves a good estimation for the compressive strength of the vertical inner plate reinforced joint.

## 1. Introduction

The application of steel square hollow section (SHS) tubular members are growing with the construction of more and more large span structures around the world [1]. A strong and reliable joint is essential for the robust of the integral structure, several reinforcement methods were thus developed during the last decades [2–4]. Amongst these methods, internal reinforcements such as stiffened rings or diaphragms, have been proved more efficient to enhance the strength of the joint than the external ones [5,6]. However, it is difficult to weld the stiffened ring inside the closed section, especially for the chord with a relatively small cross-section. To solve this problem, the external stiffened ring has been proposed and proved to be efficient to increase the compressive strength of the circle hollow section (CHS) joint [7].

The application of external stiffened ring for SHS joint is not as common as that for CHS joint, since the square chord is not as smooth as the circle section, which increases the difficulty of the cutting and welding of the stiffened ring. An alternative to use the stiffened plate externally is to weld the plate along the longitudinal direction of the chord [8–12].

There is considerable experimental or numerical data for plate-to-tubular joints. The behavior of plate-to-CHS connections was investigated experimentally by Washio et al. [13] in the early 1970s, where the test results lay the foundation for the current specification [14]. Kosteski and Packer [8,9] first studied the longitudinal branch plate-to-RHS connections, and proposed a ‘through’ branch plate to increase the strength of the connection. Afterward, Voth and Packer [15,16] conducted experimental and numerical studies of branch plate-to-CHS connections, they found that the through plate connection increased the compressive strength by more than three times than that of a branch plate connection. Based on the test data of Voth and Packer [15,16], Luis and Carlos [17] recently proposed an analytical model for the ultimate compressive strength of transversal T-type branch plate-to-CHS connections.

Although the plate-to-tubular connections are known as easy to weld, the buckling of the plate under compressive load is critical, especially for the connection with a thin and big plate [18–20]. Sheng and Yam [18] found in their FEM simulation that the ultimate loads of

* Corresponding author at: State key Laboratory of Geomechanics and Deep Underground Engineering, China University of Mining and Technology, China.
*E-mail address:* honfee@126.com (H. Chang).

https://doi.org/10.1016/j.engstruct.2018.06.036
Received 20 December 2017; Received in revised form 8 June 2018; Accepted 9 June 2018
0141-0296/ 

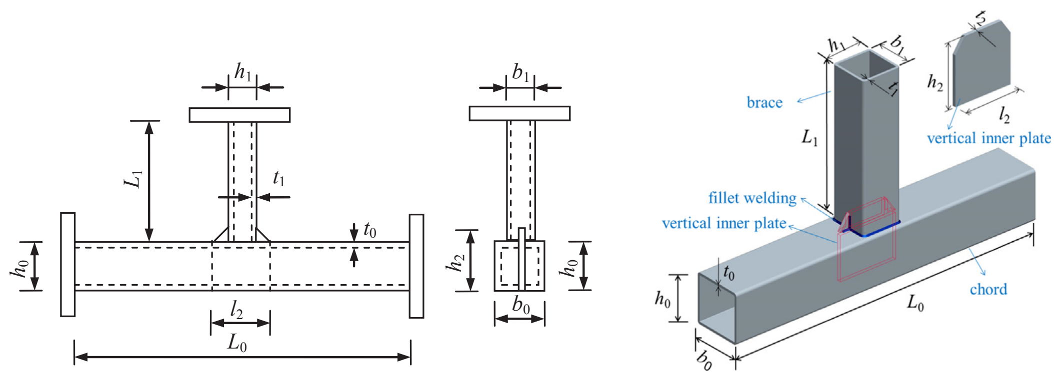


**Fig. 1.** Details of vertical inner plate reinforced square tubular T-joint (a) front view, (b) sectional view, (c) isometric drawing.

the connections decrease when the long unsupported edge length of the gusset plate is increased. The punching shear failure of the chord under tensile load for plate-to-tubular connections is another issue that needs to be noticed. Xu and Chen [21] studied the behavior of longitudinal plate-to-concrete-filled CHS connections under axial tension, eccentric tension and in-plane bending extensively. They found that the punching shear failure of the chord member was the main failure mode observed during the tests.

To alleviate the above problems, a novel vertical inner plate reinforcement (VIPR) method is developed, where the reinforcement plate is inserted into the holes cut on the flanges of the chord and the brace, and welded with them in shop, as shown in Fig. 1. Since the brace, the plate and the chord are welded together, the VIPR method is expected to decrease the risk of punching shear failure of the chord under brace tension. Meanwhile, the brace could eliminate the buckling failure of the plate under compression. Furthermore, the vertical plate is also effective to combine the top and bottom flange of the chord so as to increase the strength of the joint.

The VIPR method has been applied for the reinforcement of CHS joint previously, with the numerical studies by Wang and Zhang [22], Li and Shao [10] indicating that the vertical inner plate is effective to increase both the rigidity and the ultimate strength of the CHS joints. Zhu and Zhao [11] also found that the joint strength increased significantly as the size of the stiffener increased, and the reinforcement effect is more dependent on the stiffener length than on the stiffener height. Recently, Zhu and Song [12] proposed a theoretical formula using yield line model to predict the ultimate strength enhancement of reinforced T-joints with external stiffeners. Considering the fact that the influence of VIPR on the behavior of SHS joints is different from that of CHS joints, more experimental or numerical studies need to be conducted on VIPR SHS joints.

To this end, four SHS T-joints with and without VIPR were designed and tested herein. The experimental set-up is described and test results are discussed. Corresponding numerical models of the specimens are also developed and used to discuss the mechanism of the VIPR for SHS joints.

## 2. Experimental program

### 2.1. Details of specimens

Since the vertical inner plate is introduced to reinforce the up and bottom flange of the chord for square tubular joints, the test specimens were designed with the width ratio of $\beta \le 0.85$, which were expected to fail by the plastic failure of the chord top face. The dimensions of the vertical inner plate are designed refer to the doubler-plate as following [23]:

$$t_0 \leqslant t_2 \leqslant 1.5t_0, \quad h_0 \leqslant h_2 \leqslant 1.5h_0, \quad h_1 \leqslant l_2 \leqslant h_1 + 1.2b_0\sqrt{(1-\beta)} \tag{1}$$

where $t_0$ is the thickness of the chord, $t_2$ is the thickness of the vertical inner plate, $h_0$ is the height of the chord, $h_2$ is the height of the vertical inner plate, $h_1$ is the height of the brace, $l_2$ is the length of the vertical inner plate, $b_0$ is the width of the chord, $\beta = b_1/b_0$ is the width ratio of the brace and the chord, as shown in Fig. 1.

Four specimens with or without reinforcement were designed for the experimental test. Two unreinforced joints with the width ratio of $\beta = 0.4$ and $\beta = 0.8$ were firstly designed, with their corresponding vertical inner plate reinforced counterparts fabricated for comparison. Details of the vertical inner plate reinforced T joint are shown in Fig. 1, and the dimensions as well as the material yield strength from the coupon tests are listed in Table 1. The subscript “0”, “1” or “2” denotes a geometric or mechanical parameter of the chord, the brace and the inner-plate respectively. Other notations are defined as follows: “URT” represents an unreinforced T-joint, “IPRT” represents an inner-plate reinforced T-joint, “40” represents a brace width of 40 mm, “80” represents a brace width of 80 mm, “A” represents a static axial loading on the brace.

### 2.2. Setup of the test

The arrangements of the test specimens and the measure instruments are shown in Fig. 2. The T-joints were fixed at the two ends of the chords, and compressive load was applied at the end of the braces by an electro-hydraulic servo actuator with a maximum capacity of 1000 kN.

**Table 1**
Geometries [mm] and yield strength [N/mm$^2$] of the specimens.

| No. | Chord | | | | | Brace | | | | | Vertical inner plate | | | |
|---|---|---|---|---|---|---|---|---|---|---|---|---|---|---|
| | $b_0$ | $h_0$ | $t_0$ | $L_0$ | $f_y$ | $b_1$ | $h_1$ | $t_1$ | $L_1$ | $f_y$ | $l_2$ | $h_2$ | $t_2$ | $f_y$ |
| URT-40A | 100 | 100 | 5 | 650 | 356 | 40 | 40 | 4 | 300 | 372 | — | | | |
| IPRT-40A | 100 | 100 | 5 | 650 | 356 | 40 | 40 | 4 | 300 | 372 | 100 | 130 | 7 | 285 |
| URT-80A | 100 | 100 | 5 | 650 | 356 | 80 | 80 | 4 | 300 | 265 | — | | | |
| IPRT-80A | 100 | 100 | 5 | 650 | 356 | 80 | 80 | 4 | 300 | 265 | 120 | 130 | 7 | 285 |